

# Gene Co-Expression Network Analysis of *Trypanosoma brucei* in Tsetse Fly Vector

Kennedy W. Mwangi (✉ [wanjaukm@gmail.com](mailto:wanjaukm@gmail.com))

Jomo Kenyatta University of Agriculture and Technology

Rosaline W. Macharia

University of Nairobi

Joel L. Bargul

International Centre for Insect Physiology and Ecology, Jomo Kenyatta University of Agriculture and Technology

---

## Research

**Keywords:** *Trypanosoma brucei*, tsetse fly, gene co-expression network, weighted gene co-expression network analysis (WGCNA), 3' untranslated region (UTR)

**Posted Date:** September 18th, 2020

**DOI:** <https://doi.org/10.21203/rs.3.rs-78868/v1>

**License:** © ⓘ This work is licensed under a Creative Commons Attribution 4.0 International License.

[Read Full License](#)

---

**Version of Record:** A version of this preprint was published at Parasites & Vectors on January 22nd, 2021. See the published version at <https://doi.org/10.1186/s13071-021-04597-6>.

# Abstract

## Background

*Trypanosoma brucei* species are motile protozoan parasites that are cyclically transmitted by tsetse fly (genus *Glossina*) causing human sleeping sickness and nagana in livestock in sub-Saharan Africa. African trypanosomes display digenetic life cycle stages in the tsetse fly vector and in their mammalian host. Experimental work on insect-stage trypanosomes is challenging due to the difficulty in setting up successful *in vitro* cultures. Therefore, there is limited knowledge on the trypanosome biology during its development in the tsetse fly. Consequently, this limits the development of new strategies for blocking parasite transmission in the tsetse fly.

## Methods

In this study, RNA-Seq data of insect-stage trypanosomes were used to construct a *T. brucei* gene co-expression network using weighted gene co-expression analysis (WGCNA) method. The study identified significant enriched modules for genes that play key roles during the parasite's development in tsetse fly. Further, potential 3' untranslated region (UTR) regulatory elements for genes that clustered in the same module were identified using Finding Informative Regulatory Elements (FIRE) tool.

## Results

A fraction of gene modules (12 out of 27 modules) in the constructed network were found to be enriched in functional roles associated with cell division, protein biosynthesis, mitochondrion, and cell surface. Additionally, 12 hub genes encoding proteins such as RNA-binding protein 6 (RBP6), Arginine kinase 1 (AK1), *brucei* alanine rich protein (BARP), among others, were identified for the 12 significantly enriched gene modules. In addition, the potential regulatory elements located in the 3' untranslated regions of genes within the same module were predicted.

## Conclusions

The constructed gene co-expression network provides a useful resource for network-based data mining to identify candidate genes for functional studies. This will enhance understanding of the molecular mechanisms that underlie important biological processes during parasite's development in tsetse fly. Ultimately, these findings will be key in the identification of potential molecular targets for disease control.

## Background

*Trypanosoma brucei* has a digenetic life cycle with distinct morphological forms existing during its development in the mammalian host and the tsetse fly [1]. In the mammalian bloodstream, the morphological forms are slender and stumpy trypomastigotes, while in the tsetse fly, they comprise of procyclic trypomastigote forms in the midgut, long and short epimastigotes in the proventriculus, and

short epimastigote and metacyclic trypomastigotes in the salivary glands [2, 3]. Most *T. brucei* research has focused on the mammalian bloodstream and tsetse procyclic forms of trypanosomes as they are relatively easier to maintain in *in vitro* cultures [4, 5]. Consequently, this has led to less exploration of parasite phenotypes in the tsetse fly that could provide insights into the biology of a trypanosome during its development in the vector – the life cycle phase referred to as “the heart of darkness” [6]. The knowledge of trypanosome development in the tsetse fly will contribute to efforts towards interrupting disease transmission by the vector. This can be achieved through targeted disruption of the parasite’s essential molecular processes such as; motility, regulation of differentiation, morphological remodeling, and signal transduction [7, 8].

In the last decade, RNA-Seq technology has been a fundamental tool in studying gene expression profiles of *T. brucei* and other kinetoplastids with an aim of expanding knowledge on their biology [9]. This is because RNA-Seq provides a comprehensive and more accurate transcriptome quantification and characterization in comparison to the hybridization-based techniques such as microarray [10]. In addition to identification of differentially expressed genes, transcriptome data could also be used to create gene co-expression networks which provides a functional and molecular understanding of key biological processes in an organism [11, 12].

Gene co-expression network analysis aims to identify coordinated gene expression patterns that indicate functional relationships between the expressed genes. Using a method such as WGCNA [13], highly correlated genes are grouped into modules (or gene clusters) and are currently thought to be co-expressed, hence perform similar biological functions [14]. Each module is believed to encode a specific biological function based on the genes it contains. To associate genes in a given module to specific functions, an enrichment analysis is performed against databases such as gene ontology (GO) [15] and Kyoto Encyclopedia for Genes and Genomes (KEGG) [16].

Further, WGCNA allows identification of intra-modular hub genes which are highly connected genes in a module [13, 17]. These hub genes could play key roles in the biological functions of their modules or act as representatives of their predominant biological function [11]. Also, based on the hypothesis that functionally related genes may be co-regulated, co-expression network modules are useful in gene regulation analysis including prediction of regulatory elements (motifs) for genes in the same module [18, 19]. Additionally, functions of uncharacterized genes are predicted based on their co-expression with genes of known function in the co-expression network, a principle referred to as “guilt-by-association” [12].

The present study aimed at generation of a gene co-expression network to explore functionally relevant genes involved in *T. brucei* development in the tsetse fly vector. In contrast to a *T. brucei* gene co-expression network generated from a previous study for procyclic and bloodstream forms using microarray data [20], our study focused on the insect-stage morphological forms of the parasite by analyzing RNA-Seq data. The constructed gene co-expression network permitted identification of 12

functionally relevant modules and their 12 hub genes as well as potential regulatory motifs in the mRNA's 3' untranslated regions for genes grouped in the same module.

## Methods

### Datasets acquisition and quality assessment

RNA-Seq datasets of *Glossina morsitans morsitans* (tsetse fly) trypanosome-infected midgut, proventriculus and salivary glands tissues were obtained from European Nucleotide Archive (ENA) [21] under accession numbers SRP002243 and SRR965341. The dataset consisted of 18 samples; seven (7) midgut, four (4) proventriculus, and seven (7) salivary glands [22, 23]. The quality of the data was assessed using FastQC version 0.11.8 (<http://www.bioinformatics.babraham.ac.uk/projects/fastqc/>). Prior to reads mapping, *T. brucei* genome and *G. morsitans* scaffolds genome were obtained from TriTrypDB (Release 43) [24] and VectorBase [25], respectively, and concatenated to create a chimeric genome. The RNA-Seq reads were mapped to the chimeric genome of *T. brucei* and *G. morsitans* using HISAT2 version 2.1.0 [26] to remove ambiguously mapped reads. Duplication rates were computed after read mapping using MarkDuplicates tool from Picard toolkit version 2.20.3 (<http://broadinstitute.github.io/picard/>) to mark duplicate reads. Further, dupRadar Bioconductor R package version 1.18.0 was used to assess the RNA-Seq data for presence of PCR duplicates [27]. Samples that had PCR duplicates were excluded from downstream analysis.

### Reads quantification

The reads that mapped to *T. brucei* genome were counted using HTSeq version 0.11.2 [28] using the annotation file of *T. brucei* downloaded from TriTrypDB (Release 43). Non-protein coding genes (ncRNA, snRNA, snoRNA, pseudogenic transcripts, rRNA and tRNA) were excluded from the read counts as this study focused on protein-coding genes and their functional analysis.

### Sample quality assessment and filtering

Genes with low expression levels were removed from the read counts data using *filterByExpr* function from R package edgeR version 3.8 [29]. Sample quality was assessed using Pearson correlation heatmaps, and Principal Component Analysis (PCA) and box plots in R version 3.6.0 [30]. Trimmed mean of M-values (TMM) was used as a normalization method using *calcNormFactors* function in edgeR [29]. The normalized read counts were then converted to counts per million and  $\log_2$  transformed for downstream analysis. Batch effects were adjusted for using ComBat method from sva R package version 3.32.1 [31].

### Construction of the weighted gene co-expression network

The weighted gene co-expression network was constructed using WGCNA R package version 1.66 [17]. First, soft-thresholding power,  $\beta$ , was determined using *pickSoftThreshold* function from WGCNA

package. This was followed by the construction of a weighted adjacency matrix using *adjacency* function, after which the matrix was computed into Topological Overlap Matrix (TOM) using the *TOMsimilarity* function [13]. The TOM measure between pairs of genes was used as input for average linkage hierarchical clustering by first creating a dissimilarity matrix ( $\text{dissTOM} = 1 - \text{TOM}$ ) and then using *flashClust* function to create the gene tree dendrogram. The Dynamic Tree Cut algorithm was used to identify modules using the gene tree dendrogram as input for *cutreeDynamicTree* function from dynamicTreeCut R package version 1.63-1 [32]. The *chooseTopHubInEachModule* function from WGCNA package was used to identify the hub genes.

## Network functional enrichment analysis and visualization

The goseq R package version 1.36.0 [33] was used to test for enrichment of gene ontology (GO) [15] and Kyoto Encyclopedia of Gene and Genomes (KEGG) [16] annotations for each of the identified modules. The GO and KEGG annotations were obtained from TriTrypDB. The generated lists of GO terms for the modules were summarized using REVIGO (<http://revigo.irb.hr/>) [34]. Cytoscape version 3.7.1 [35] was used to visualize the network using the *exportNetworkToCytoscape* function from WGCNA package.

## Prediction of 3' UTR regulatory motifs

All the genes in the gene co-expression network and their corresponding cluster/module index were used to generate an expression file that was used as input for the tool FIRE, version 1.1a [19]. This expression file was submitted online to FIRE (<https://tavazoielab.c2b2.columbia.edu/FIRE/>) with default parameters for prediction of 3' UTR motifs.

The code used in data pre-processing, network construction, and functional analysis is provided here as Additional file 1 and archived at: [https://github.com/wanjauk/tbrucei\\_gcn](https://github.com/wanjauk/tbrucei_gcn). Motif prediction was performed online at: <https://tavazoielab.c2b2.columbia.edu/FIRE/>.

# Results

## Data pre-processing

A total of 18 samples of raw RNA-Seq data (Additional file 2: Table S1) were obtained for this study. Out of the 18 samples, three (3) of them generated from the trypanosome-infected salivary glands were excluded from further analysis because they contained PCR duplicates. Thus, a total of 15 samples were analyzed (Additional file 2: Table S1). Further, lowly expressed genes were excluded in order to reduce noise, thus resulting in a total of 7,390 genes across the 15 samples.

The relationship between the samples and the reproducibility of biological replicates was determined using Principal Component Analysis (PCA) and Pearson correlation heatmap analysis prior to (Additional file 3: Figure S1) and after adjusting for batch effects which could have resulted from biological replicates (Fig. 1). The PCA and Pearson correlation heatmap plots showed that the samples grouped together based on the developmental stages of *T. brucei* in the insect vector rather than their biological

replicates (Fig. 1). An assessment of the distribution of per-gene read counts per sample showed a median steady-state expression level of  $\sim 6.5 \log_2$  counts per million in all the 15 samples (Additional file 4: Figure S2).

### **Weighted gene co-expression network construction**

A total of 7,390 protein coding genes from 15 samples were used for the construction of the co-expression network. Prior to generation of the network, the soft-thresholding power to which co-expression similarity was raised to calculate adjacency was determined by analysis of thresholding powers from 1 to 20. Power 14, the power for which the scale-free topology fitting index ( $R^2$ ) was  $\geq 0.8$ , was chosen (Additional file 5: Figure S3). A total of 28 distinct modules were generated for 7,390 protein coding genes from the hierarchical clustering tree (dendrogram) using the dynamic tree cut algorithm (Figure 2, Figure 3, and Additional file 6). The grey module, which contained 59 genes that could not be assigned to any module, was excluded from the analysis (Figure 3). Thus, a total of 27 modules were used in subsequent analysis. The module with the least genes was the white module with 61 genes while the turquoise module had the largest number of genes with 732 genes (Figure 3).

### **Functional and pathway enrichment analysis**

Out of the 27 modules generated, only 14 modules were found to be enriched for GO terms; 12 were over-represented and two (2) (blue and green modules) were under-represented for GO terms (Additional file 7). Seven (7) out of the 27 modules were enriched following KEGG pathway enrichment analysis, from which five (5) were over-represented and two (2) (lightcyan and blue modules) were under-represented for KEGG pathway terms (Additional file 8). The top enriched GO terms for the modules with over-represented GO terms highlights some functions of the module genes (Table 1). Out of the 12 modules with over-represented GO terms, four (4) modules were over-represented for KEGG pathway terms and one module (yellow module) was over-represented for a KEGG pathway term (endocytosis), but not GO terms (Table 1).

Table 1

Modules with over-represented GO terms and their most significant over-represented GO and KEGG pathway terms.

Module	Top Enriched GO term	GO term adjusted $p$ -value	KEGG pathways term	KEGG term adjusted $p$ -value
Brown	Adenylate cyclase activity	1.151E-02		
Black	Cellular nitrogen compound biosynthetic process	2.779E-07		
Pink	Cytochrome complex	4.917E-02	RNA transport	3.187E-02
Darkturquoise	Transferase activity, transferring phosphorus-containing groups	1.815E-02		
Salmon	RNA binding	2.191E-03		
Purple	Mitochondrial protein complex	1.093E-06		
Lightyellow	Structural constituent of ribosome	6.262E-11	Ribosome	9.416E-08
Turquoise	Cell surface	2.395E-04		
Red	Cytoskeletal part	7.976E-04	Homologous recombination	1.478E-02
Tan	Spindle pole	4.930E-02		
Greenyellow	Cytoskeleton	1.211E-03		
Magenta	Cytoskeleton	3.979E-04	Purine metabolism	9.042E-03
Yellow			Endocytosis	2.502E-02
"_" indicates detection of no significant GO or KEGG terms.				

### Modules hub gene identification

Highly connected genes in a module are referred to as intra-modular hub genes. These hub genes are considered functionally significant in the enriched functions of the modules. Following the hypothesis that higher connectivity for a gene implies more importance in the module's functional role, genes with the highest connectivity in the 27 modules were determined and considered to be the hub genes (Additional file 9). Hub genes for the 12 modules with over-represented GO terms are shown in Table 2.

Table 2  
Identified hub genes and their encoding proteins for the 12 modules with over-represented GO terms.

Module	Hub gene	Encoding protein
Brown	Tb927.11.1570	Hypothetical protein, conserved
Black	Tb927.7.1790	Adenine phosphoribosyltransferase, putative
Pink	Tb927.10.6200	Hypothetical protein, conserved
Darkturquoise	Tb927.8.6650	RNA-binding protein, putative
Salmon	Tb927.11.1450	2-oxoglutarate dehydrogenase E1 component, putative
Purple	Tb927.1.600	Phosphate-repressible phosphate permease, putative
Lightyellow	Tb927.10.2560	Mitochondrial malate dehydrogenase
Red	Tb927.7.6920	Hypothetical protein, conserved
Tan	Tb927.3.2930	RNA-binding protein RBP6, putative
Greenyellow	Tb927.7.920	Inner arm dynein 5 - 1
Magenta	Tb927.9.6290	Arginine kinase
Turquoise	Tb927.9.15630	BARP protein

### 3' UTR motif prediction based on gene co-expression modules

Genes in a given module are hypothesized to be co-regulated as they are assumed to have similar functions. Consequently, their *cis*-regulatory element should be similar. Following this hypothesis, a total of 10 statistically significant RNA motifs each over-represented in different gene modules were identified using FIRE (Figure 4a).

## Discussion

This study employed the WGCNA method [17] to construct the *T. brucei* weighted gene co-expression network using RNA-Seq data. The resulting co-expression network analysis allowed identification of modules (gene clusters) as well as enrichment analysis in GO [15] and KEGG [16] annotation databases to associate the modules with their functions. Highly connected genes in a module, known as intra-modular hub genes [17], were also determined as they are key drivers of a molecular process or act as a representative of the predominant biological function of the module. Here, we demonstrate the usefulness of the network for functional genomic analysis using an example of the cell cycle and protein biosynthesis enriched functions.

The cell cycle in eukaryotes comprises of four phases, namely:  $G_0/G_1$ , S,  $G_2$ , and M phases [36]. The cell prepares for division in the first gap phase ( $G_0/G_1$ ), replicates the DNA during the S phase, and then undergoes mitosis (M) in the second gap phase ( $G_2$ ). In *T. brucei*, the cell cycle is tightly regulated to ensure that single-copy organelles and structures such as Golgi body, mitochondrion, kinetoplast, nucleus, basal body, and flagellum are duplicated, maintained at precise positions in the cell and segregated accurately [37]. Various GO terms related to organelles were over-represented in the black module (Figs. 2 and 3) and included microbody, peroxisome, glycosome, and acidocalcisome (Additional file 10: Figure S4). The organelles duplicate in the first gap phase ( $G_0/G_1$ ) [38]. This suggests that genes assigned to the black module (Figs. 2 and 3) could play a role in the cell cycle particularly during the  $G_0/G_1$  phase. Furthermore, some cyclins and cdc2-related kinases (CRKs) that are key regulators of cell cycle such as CYC2 (Tb927.11.14080), CYC5 (Tb927.10.11440), and CRK10 (Tb927.3.4670) were assigned to the black module (Additional file 6). CY2 and CY5 regulate transition of  $G_1$  phase to S phase [39]. Co-expression of CRK10, whose regulatory role is presently unknown, with CYC2 and CYC5 and its demonstrated interaction with CYC2 in yeast two-hybrid assay [39], suggests a possible role in  $G_1$  to S phase transition.

The hub gene for the black module was identified as adenine phosphoribosyltransferase (APRT) (Table 2) that plays a crucial role in purine salvage pathway in *T. brucei*. This parasite lacks *de novo* purine biosynthetic pathway [40]. Purine nucleotides are precursors of DNA and RNA and are also constituents of second messengers in signaling pathways such as cyclic AMP [41]. In this regard, APRT may be important in enriched module functions such as cyclic nucleotide biosynthesis and synthesis of structural constituent of the ribosome particularly ribosomal RNA, and consequently, signaling and protein biosynthesis. Signaling is depicted by the black module's over-represented GO terms such as adenylate cyclase activity, while protein biosynthesis is depicted by GO terms such as translation, unfolded protein binding, protein folding, and structural constituent of ribosome (Additional file 10: Figure S4).

The red module (Figs. 2 and 3) was functionally enriched for GO terms such as DNA replication and chromosome organization, and KEGG pathway term homologous recombination indicating that its genes are involved in the progression of cell cycle (Additional file 11: Figure S5 and Table 1). Additionally, the red module has some genes involved in cytokinesis such as BOH1 (Tb927.10.12720), that cooperates with *TbPLK* to initiate cytokinesis and flagellum inheritance [42], and Cytokinesis Initiation Factor 2 (CIF2) (Tb927.9.14290) which is involved in initiation of cytokinesis [43] (Additional file 6). Other genes assigned to this module were in concordance with the enriched functions. These were nucleus- and spindle-associated protein 1 (NuSAP1) (Tb927.11.8370) that is required in chromosome segregation and NuSAP2 (Tb927.9.6110) that promotes  $G_2/M$  transition [44]. The hub gene for the red module is a hypothetical gene (Tb927.7.6920) which may play a key role in the progression of cell cycle.

The tan module (Figs. 2 and 3), whose enriched GO terms include spindle pole and microtubule cytoskeleton, has genes such as CIF4 (Tb927.10.8240), TLK1 (Tb927.4.5180) and FPRC (Tb927.10.6360)

that are involved in cytokinesis [45, 46]. The hub gene for the tan module is RNA-binding protein RBP6 (Table 2). Interestingly, over-expression of RBP6 *in vitro* has been demonstrated to recapitulate the parasite's tsetse fly stage developmental form that were previously elusive in culture [47]. However, the exact role of RBP6 during the parasite's development in the tsetse fly is yet to be elucidated. Based on its assignment to the tan module, it is likely to be involved in regulating a key step during progression of the cell cycle.

The salmon module (Figs. 2 and 3) has enriched functions in RNA metabolic processing depicted by the module's enriched GO terms which are RNA metabolism, nucleic acid binding, and RNA binding (Additional file 12: Figure S6). RNA binding may either involve binding of the mRNA by RNA-binding proteins (RBPs) as a post-transcriptional gene regulation mechanism in *T. brucei* [48, 49], or binding by translation initiation factors for protein synthesis [50]. The salmon module has translation initiation factor eIF4E1 (Tb927.11.2260) and poly(A) binding protein PABP2 (Tb927.9.10770) that have previously been shown to have similar co-localization in *T. brucei* [51]. An RNA-binding protein related to stress response, ZC3H30 (Tb927.10.1540), together with an associated stress response granule (Tb927.8.3820) [52], were assigned to the salmon module. The hub gene for the salmon module is 2-oxoglutarate dehydrogenase E1 component (Table 2). The 2-oxoglutarate dehydrogenase is an enzyme involved in the tricarboxylic acid cycle (TCA) in the mitochondrion implicated in the degradation of proline and glutamate to succinate which can enter gluconeogenesis pathway in procyclic trypanosomes [53]. This hub gene could be important in the role of the mitochondrion in responding to stress as a result of change in energy source in insect-stage trypanosomes.

Regulation of gene expression in *T. brucei* occurs almost exclusively post-transcriptionally as a result of polycistronic arrangement of their genes [50, 54, 55]. Post-transcriptional regulation of mRNA abundance mainly involves interaction of their *cis*-regulatory element and a *trans*-acting element such as an RNA-binding protein [56]. Genes with similar functions are co-regulated together thus their mRNAs are hypothesized to have similar *cis*-regulatory elements [19]. Since the gene modules of a co-expression network are composed of genes with similar functions, they can be used as a basis for identifying potential regulatory elements in the untranslated regions of mRNA.

Two motifs ([AU]A[CGU]AUGUA[CGU] and [CGU][CU]AUAGA.[ACU]) that had consensus sequences similar to previously identified motifs were found to be over-represented (Fig. 4a). The motif [AU]A[CGU]AUGUA[CGU] contains the core sequence, UGUA, that is recognized by the PUF family of RNA-binding proteins [57] and has previously been identified in *T. brucei* as targeting transcripts involved in the cell cycle [58–60]. The motif was over-represented in the black, pink and darkturquoise modules (Fig. 4a). [AU]A[CGU]AUGUA[CGU] co-occurs with other motifs which are [CGU]AAU.[AU]UA., .UUUUUA., [AC]GGA[AG]U[AG]A. and [AGU]UUUGGUU[AGU] (lighter colors in Fig. 4b). Co-occurrence of motifs means that they either co-localize within the same untranslated region (UTR) which indicates that the presence of one motif implies presence of its putative counterpart [19]. These co-occurring motifs may provide further information on post-transcriptional regulation. For instance, co-localization of two motifs close to

each other on a transcript could imply physical interaction of their binding elements, hence their functional interaction [19].

The other motif, [CGU][CU]AUAGA.[ACU], was over-represented in the red and greenyellow modules (Fig. 4a). This consensus motif contains the core AUAGA sequence similar to CAUAGAA that has been implicated in cell cycle regulation [61, 62] and was previously predicted in *T. brucei* [60]. Notably, genes in the red module were enriched for cell cycle functions while those in the greenyellow module were enriched for microtubule associated functions, including motility (Additional file 13: Figure S7). Motility in *T. brucei* is mediated through the flagellum [63]. Importantly, flagellum motility is essential for completion of the cell division [64, 65] suggesting co-regulation of genes in the greenyellow module together with those in the red module. The motif [CGU][CU]AUAGA.[ACU] does not co-occur with other motifs which possibly suggests that its functions have opposing effects compared with functions of the other motifs (Fig. 4b). Overall, characterization of these identified *cis*-regulatory elements will advance our knowledge on post-transcription gene regulation and provide potential chemotherapeutic targets against key regulatory functions in *T. brucei* for disease control.

## Conclusions

Construction of the *T. brucei* gene co-expression network provides a valuable resource for identifying candidate genes for experimental work. These candidate genes could be important in elucidating molecular mechanisms that underlie important biological processes during the parasite's development in tsetse fly. Our results indicate correspondence between the enriched functions of module genes and known *T. brucei* biology, therefore, illustrating the effectiveness of the co-expression network analysis as an approach to explore functionally relevant genes in *T. brucei* development in tsetse fly. Knowledge on *T. brucei* development in the tsetse fly vector is crucial in identifying key targets to block transmission of these medically and economically important parasites.

## Abbreviations

**AK1:** Arginine kinase 1

**APRT:** Adenine phosphoribosyltransferase

**BARP:** Brucei alanine rich protein

**BOH1:** Bait on hook 1

**CIF:** Cytokinesis initiation factor

**CRK:** cdc2-related kinase

**ENA:** European nucleotide archive

**FIRE:** Finding informative regulatory elements

**GO:** Gene ontology

**KEGG:** Kyoto encyclopedia of genes and genomes

**PABP:** Poly(A) binding protein

**PCA:** Principal component analysis

**RBP6:** RNA-binding protein 6

**TMM:** Trimmed mean of M-values

**TOM:** Topological overlap matrix

**UTR:** Untranslated region

**WGCNA:** Weighted gene correlation network analysis

## **Declarations**

### **Ethics approval and consent to participate**

Not applicable

### **Consent for publication**

Not applicable

### **Availability of data and materials**

The datasets supporting the conclusions of this study are included within the article and in the additional data files.

### **Competing interests**

The authors declare that they have no competing interests

### **Funding**

This work was supported through the DELTAS Africa Initiative grant # DEL-15-011 to THRiVE-2. The DELTAS Africa Initiative is an independent funding scheme of the African Academy of Sciences (AAS)'s Alliance for Accelerating Excellence in Science in Africa (AESA) and supported by the New Partnership for Africa's Development Planning and Coordinating Agency (NEPAD Agency) with funding from the Wellcome Trust grant # 107742/Z/15/Z and the UK government. The views expressed in this publication

are those of the author(s) and not necessarily those of AAS, NEPAD Agency, Wellcome Trust or the UK government.

### **Authors' contributions**

KWM, RWM, JLB conceived and designed experiments.

KWM performed experiments.

RWM, JLB contributed reagents/materials/analysis tools.

KWM, RWM, JLB analyzed data.

KWM wrote the first manuscript draft.

All authors read and approved the final version

### **Acknowledgements**

We thank Dr Caleb Kibet for his technical assistance during the study, and Dr Dan Masiga and Dr Jandouwe Villinger for insightful comments during the course of the study.

## **References**

1. Vickerman K. Developmental cycles and biology of pathogenic trypanosomes. *Br Med Bull.* 1985;41:105–14.
2. Sharma R, Peacock L, Gluenz E, Gull K, Gibson W, Carrington M. Asymmetric cell division as a route to reduction in cell length and change in cell morphology in trypanosomes. *Protist.* 2008;159:137–51.
3. Dyer NA, Rose C, Ejeh NO, Acosta-Serrano A. Flying tryps: survival and maturation of trypanosomes in tsetse flies. *Trends Parasitol.* 2013;29:188–96.
4. Brun R, Schönenberger null. Cultivation and in vitro cloning or procyclic culture forms of *Trypanosoma brucei* in a semi-defined medium. Short communication. *Acta Trop.* 1979;36:289–92.
5. Hirumi H, Doyle JJ, Hirumi K. Cultivation of bloodstream *Trypanosoma brucei*. *Bull World Health Organ.* 1977;55:405–9.
6. Sharma R, Gluenz E, Peacock L, Gibson W, Gull K, Carrington M. The heart of darkness: growth and form of *Trypanosoma brucei* in the tsetse fly. *Trends Parasitol.* 2009;25:517–24.
7. Ooi C-P, Bastin P. More than meets the eye: understanding *Trypanosoma brucei* morphology in the tsetse. *Front Cell Infect Microbiol.* 2013;3:71.
8. Abbeele JVD, Rotureau B. New insights in the interactions between African trypanosomes and tsetse flies. *Front Cell Infect Microbiol.* 2013;3:63.

9. Patino LH, Ramírez JD. RNA-Seq in kinetoplastids: A powerful tool for the understanding of the biology and host-pathogen interactions. *Infect Genet Evol J Mol Epidemiol Evol Genet Infect Dis*. 2017;49:273–82.
10. Marioni JC, Mason CE, Mane SM, Stephens M, Gilad Y. RNA-Seq: an assessment of technical reproducibility and comparison with gene expression arrays. *Genome Res*. 2008;18:1509–17.
11. Barabási A-L, Oltvai ZN. Network biology: understanding the cell’s functional organization. *Nat Rev Genet*. 2004;5:101–13.
12. Wolfe CJ, Kohane IS, Butte AJ. Systematic survey reveals general applicability of “guilt-by-association” within gene coexpression networks. *BMC Bioinformatics*. 2005;6:227.
13. Zhang B, Horvath S. A general framework for weighted gene co-expression network analysis. *Stat Appl Genet Mol Biol*. 2005;4:Article 17.
14. van Dam S, Vösa U, van der Graaf A, Franke L, de Magalhães JP. Gene co-expression analysis for functional classification and gene–disease predictions. *Brief Bioinform*. 2018;19:575–92.
15. Ashburner M, Ball CA, Blake JA, Botstein D, Butler H, Cherry JM, et al. Gene Ontology: tool for the unification of biology. *Nat Genet*. 2000;25:25–9.
16. Kanehisa M, Goto S. KEGG: Kyoto Encyclopedia of Genes and Genomes. *Nucleic Acids Res*. 2000;28:27–30.
17. Langfelder P, Horvath S. WGCNA: an R package for weighted correlation network analysis. *BMC Bioinformatics*. 2008;9:559.
18. van Helden J, André B, Collado-Vides J. Extracting regulatory sites from the upstream region of yeast genes by computational analysis of oligonucleotide frequencies. *J Mol Biol*. 1998;281:827–42.
19. Elemento O, Slonim N, Tavazoie S. A universal framework for regulatory element discovery across all genomes and data-types. *Mol Cell*. 2007;28:337–50.
20. Shateri Najafabadi H, Salavati R. Functional Genome Annotation by Combined Analysis across Microarray Studies of *Trypanosoma brucei*. *PLoS Negl Trop Dis*. 2010;4:e810.
21. Leinonen R, Akhtar R, Birney E, Bower L, Cerdeno-Tárraga A, Cheng Y, et al. The European Nucleotide Archive. *Nucleic Acids Res*. 2011;39:D28–31.
22. Telleria EL, Benoit JB, Zhao X, Savage AF, Regmi S, e Silva TLA, et al. Insights into the Trypanosome-Host Interactions Revealed through Transcriptomic Analysis of Parasitized Tsetse Fly Salivary Glands. *PLoS Negl Trop Dis*. 2014;8:e2649.
23. Savage AF, Kolev NG, Franklin JB, Vigneron A, Aksoy S, Tschudi C. Transcriptome Profiling of *Trypanosoma brucei* Development in the Tsetse Fly Vector *Glossina morsitans*. *PLoS One*. 2016;11:e0168877.
24. Aslett M, Aurrecochea C, Berriman M, Brestelli J, Brunk BP, Carrington M, et al. TriTrypDB: a functional genomic resource for the Trypanosomatidae. *Nucleic Acids Res*. 2010;38:D457–62.
25. Lawson D, Arensburger P, Atkinson P, Besansky NJ, Bruggner RV, Butler R, et al. VectorBase: a home for invertebrate vectors of human pathogens. *Nucleic Acids Res*. 2007;35:D503–5.

26. Kim D, Langmead B, Salzberg SL. HISAT: a fast spliced aligner with low memory requirements. *Nat Methods*. 2015;12:357–60.
27. Sayols S, Scherzinger D, Klein H. dupRadar: a Bioconductor package for the assessment of PCR artifacts in RNA-Seq data. *BMC Bioinformatics*. 2016;17:428.
28. Anders S, Pyl PT, Huber W. HTSeq—a Python framework to work with high-throughput sequencing data. *Bioinformatics*. 2015;31:166–9.
29. Robinson MD, McCarthy DJ, Smyth GK. edgeR: a Bioconductor package for differential expression analysis of digital gene expression data. *Bioinformatics*. 2010;26:139–40.
30. R Core Team. R: A Language and Environment for Statistical Computing [Internet]. Vienna, Austria: R Foundation for Statistical Computing; 2019. Available from: <https://www.r-project.org/>
31. Leek JT, Johnson WE, Parker HS, Jaffe AE, Storey JD. The sva package for removing batch effects and other unwanted variation in high-throughput experiments. *Bioinformatics*. 2012;28:882–3.
32. Langfelder P, Zhang B, Horvath S. Defining clusters from a hierarchical cluster tree: the Dynamic Tree Cut package for R. *Bioinformatics*. 2008;24:719–20.
33. Young MD, Wakefield MJ, Smyth GK, Oshlack A. Gene ontology analysis for RNA-Seq: accounting for selection bias. *Genome Biol*. 2010;11:R14.
34. Supek F, Bošnjak M, Škunca N, Šmuc T. REVIGO Summarizes and Visualizes Long Lists of Gene Ontology Terms. *PLoS ONE*. 2011;6:e21800.
35. Shannon P, Markiel A, Ozier O, Baliga NS, Wang JT, Ramage D, et al. Cytoscape: A Software Environment for Integrated Models of Biomolecular Interaction Networks. *Genome Res*. 2003;13:2498–504.
36. Hammarton TC. Cell cycle regulation in *Trypanosoma brucei*. *Mol Biochem Parasitol*. 2007;153:1–8.
37. Wheeler RJ, Gull K, Sunter JD. Coordination of the Cell Cycle in Trypanosomes. *Annu Rev Microbiol*. 2019;73:133–54.
38. Zhou Q, Hu H, Li Z. New Insights into the Molecular Mechanisms of Mitosis and Cytokinesis in Trypanosomes. *Int Rev Cell Mol Biol*. 2014;308:127–66.
39. Liu Y, Hu H, Li Z. The cooperative roles of PHO80-like cyclins in regulating the G1/S transition and posterior cytoskeletal morphogenesis in *Trypanosoma brucei*. *Mol Microbiol*. 2013;90:130–46.
40. Hammond DJ, Gutteridge WE. Purine and pyrimidine metabolism in the trypanosomatidae. *Mol Biochem Parasitol*. 1984;13:243–61.
41. Ślepokura KA. Purine 3':5'-cyclic nucleotides with the nucleobase in a *syn* orientation: cAMP, cGMP and cIMP. *Acta Crystallogr Sect C Struct Chem*. 2016;72:465–79.
42. Pham KTM, Zhou Q, Kurasawa Y, Li Z. BOH1 cooperates with Polo-like kinase to regulate flagellum inheritance and cytokinesis initiation in *Trypanosoma brucei*. *J Cell Sci*. 2019;132.
43. Zhou Q, Hu H, Li Z. An EF-hand-containing Protein in *Trypanosoma brucei* Regulates Cytokinesis Initiation by Maintaining the Stability of the Cytokinesis Initiation Factor CIF1. *J Biol Chem*. 2016;291:14395–409.

44. Zhou Q, Lee KJ, Kurasawa Y, Hu H, An T, Li Z. Faithful chromosome segregation in *Trypanosoma brucei* requires a cohort of divergent spindle-associated proteins with distinct functions. *Nucleic Acids Res.* 2018;46:8216–31.
45. Li Z, Umeyama T, Wang CC. The Chromosomal Passenger Complex and a Mitotic Kinesin Interact with the Tousled-Like Kinase in Trypanosomes to Regulate Mitosis and Cytokinesis. *PLOS ONE.* 2008;3:e3814.
46. Hu H, An T, Kurasawa Y, Zhou Q, Li Z. The trypanosome-specific proteins FPRC and CIF4 regulate cytokinesis initiation by recruiting CIF1 to the cytokinesis initiation site. *J Biol Chem.* 2019;294:16672–83.
47. Kolev NG, Ramey-Butler K, Cross GAM, Ullu E, Tschudi C. Developmental Progression to Infectivity in *Trypanosoma brucei* Triggered by an RNA-Binding Protein. *Science.* 2012;338:1352–3.
48. Clayton C. The Regulation of Trypanosome Gene Expression by RNA-Binding Proteins. *PLoS Pathog.* 2013;9:e1003680.
49. Kolev NG, Ullu E, Tschudi C. The emerging role of RNA-binding proteins in the life cycle of *Trypanosoma brucei*. *Cell Microbiol.* 2014;16:482–9.
50. Clayton C, Shapira M. Post-transcriptional regulation of gene expression in trypanosomes and leishmanias. *Mol Biochem Parasitol.* 2007;156:93–101.
51. Kramer S, Bannerman-Chukualim B, Ellis L, Boulden EA, Kelly S, Field MC, et al. Differential Localization of the Two *T. brucei* Poly(A) Binding Proteins to the Nucleus and RNP Granules Suggests Binding to Distinct mRNA Pools. *PLoS ONE.* 2013;8:e54004.
52. Chakraborty C, Clayton C. Stress susceptibility in *Trypanosoma brucei* lacking the RNA-binding protein ZC3H30. *PLoS Negl Trop Dis.* 2018;12:e0006835.
53. van Weelden SWH, van Hellemond JJ, Opperdoes FR, Tielens AGM. New functions for parts of the Krebs cycle in procyclic *Trypanosoma brucei*, a cycle not operating as a cycle. *J Biol Chem.* 2005;280:12451–60.
54. Clayton CE. Life without transcriptional control? From fly to man and back again. *EMBO J.* 2002;21:1881–8.
55. Queiroz R, Benz C, Fellenberg K, Hoheisel JD, Clayton C. Transcriptome analysis of differentiating trypanosomes reveals the existence of multiple post-transcriptional regulons. *BMC Genomics.* 2009;10:495.
56. Haile S, Papadopoulou B. Developmental regulation of gene expression in trypanosomatid parasitic protozoa. *Curr Opin Microbiol.* 2007;10:569–77.
57. Gerber AP, Luschnig S, Krasnow MA, Brown PO, Herschlag D. Genome-wide identification of mRNAs associated with the translational regulator PUMILIO in *Drosophila melanogaster*. *Proc Natl Acad Sci U S A.* 2006;103:4487–92.
58. Archer SK, Luu V-D, de Queiroz RA, Brems S, Clayton C. *Trypanosoma brucei* PUF9 Regulates mRNAs for Proteins Involved in Replicative Processes over the Cell Cycle. *PLoS Pathog.* 2009;5:e1000565.



left side of the sample correlation heatmap indicate samples based on the batch they belong to. MG1 and MG2 are midgut samples, PV2 are proventriculus samples, and SA2 are salivary gland samples.

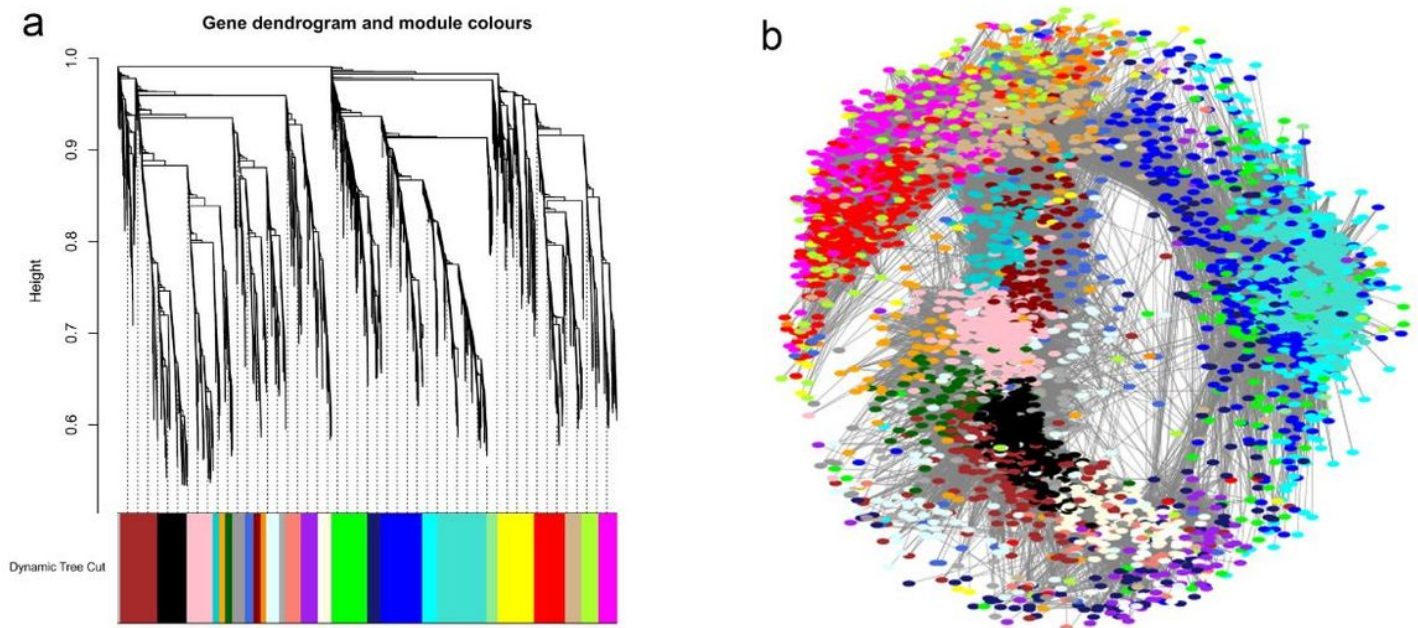


**Figure 2**

An illustration of the identified gene co-expression network modules in *T. brucei*. (a) Hierarchical cluster dendrogram. The x-axis represents co-expression distance of the genes, while the y-axis represents the genes. A dynamic tree cutting algorithm identified the modules by splitting the tree at significant branching points. Modules are represented by different colors as shown by the dendrogram. (b) Co-expression network from weighted gene co-expression network analysis (WGCNA) based on topological overlap measure (TOM) greater than 0.3 for visualization. Each point (or node) on the network represents a gene and points of the same color form a gene module. Lines (edges) on the network connecting the nodes represents a relationship between the genes.

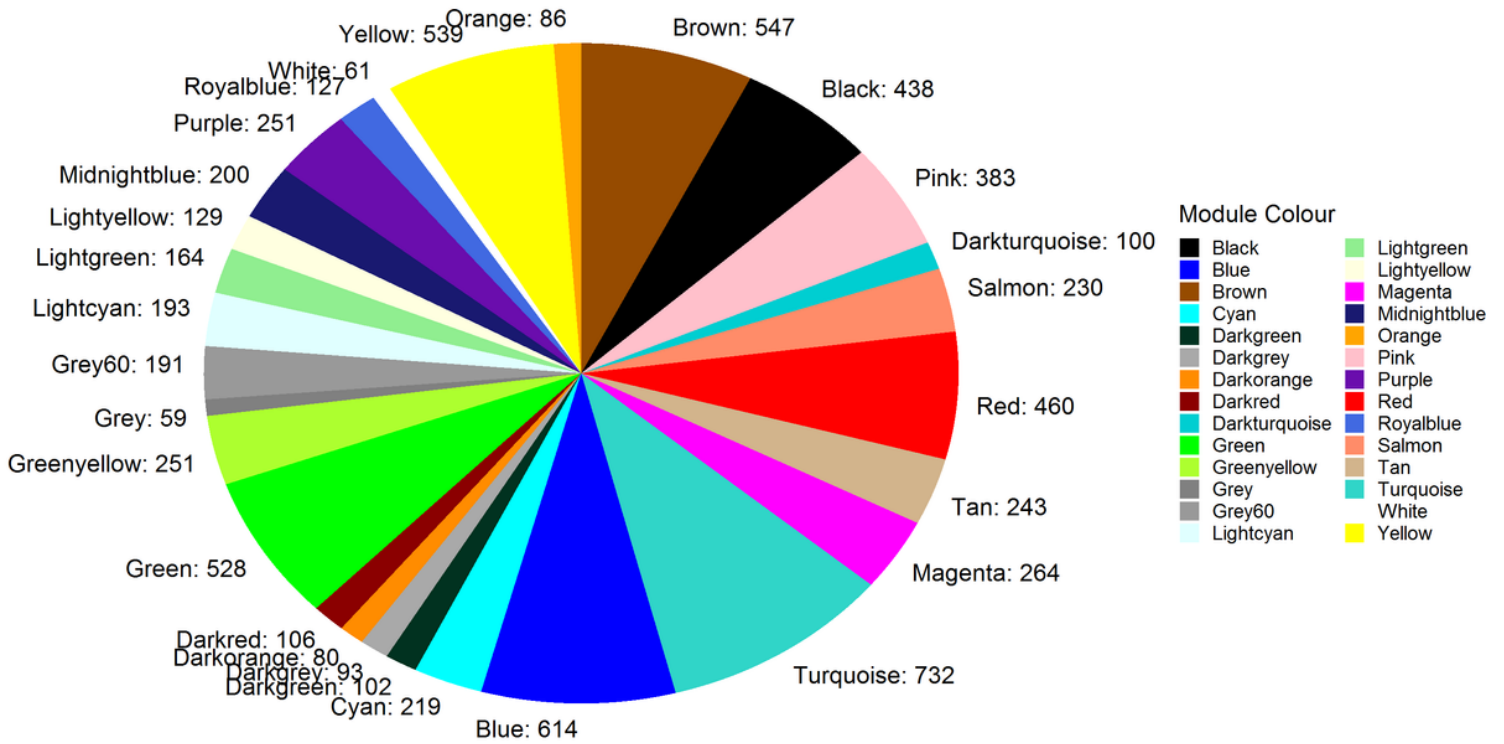


**Figure 3**

Number of genes identified in each module. In total, there were 28 modules. The grey module contains 59 genes that could not be assigned to any module and was excluded from downstream analysis.

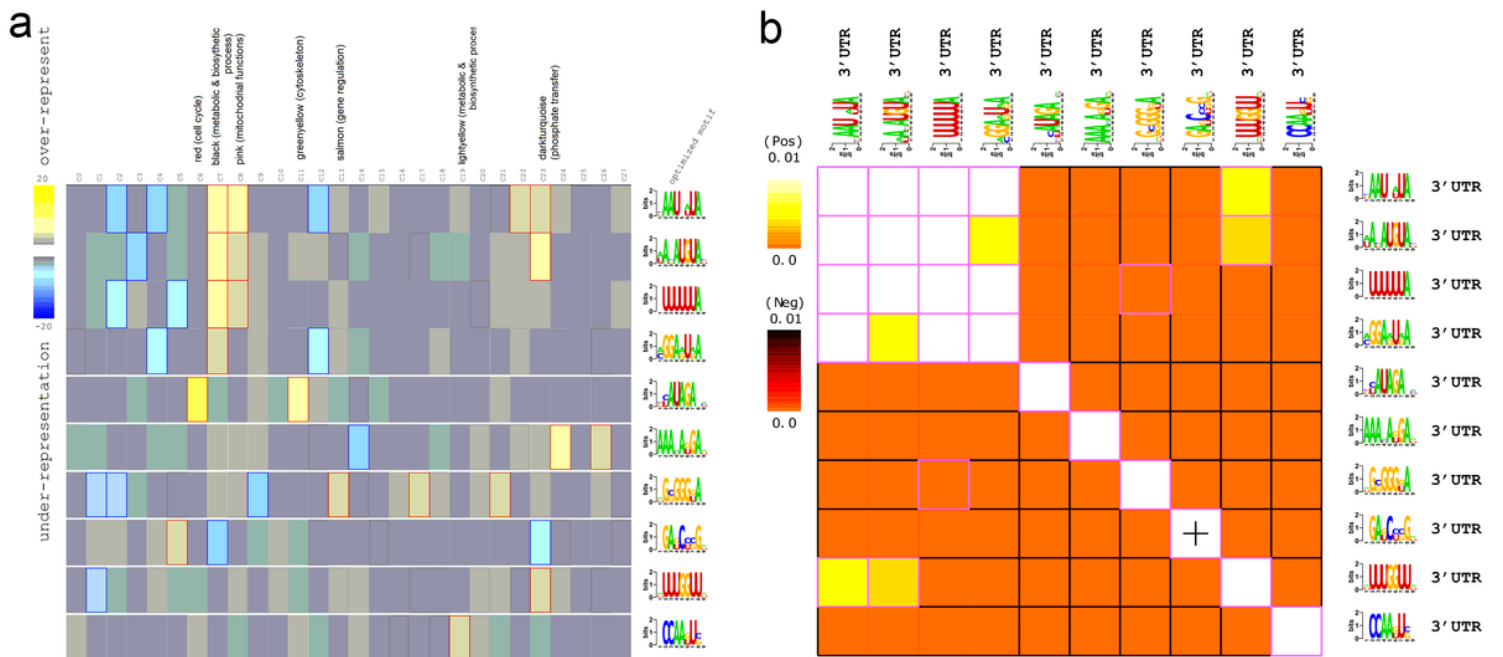


**Figure 4**

Prediction of regulatory elements in the 3' untranslated regions (UTR) based on gene co-expression modules. (a) Predicted motifs for the gene modules are shown. Columns represent gene modules, while rows represent the predicted motifs with consensus sequence on the right side. Over-representation of a

motif for a given gene module is indicated by yellow color with significant over-representation highlighted by red frames. Blue color map and frames indicate under-representation. (b) Motif pairs co-occurring in the 3' UTR are shown in the heatmap where each row and each column correspond to a predicted motif. Light colors indicate presence of another motif within the same 3' UTR while dark colors indicate that the motifs are absent in the same 3' UTR. "+" indicates significant spatial co-localization between pairs of motifs.

## Supplementary Files

This is a list of supplementary files associated with this preprint. Click to download.

- [Additionalfile1.pdf](#)
- [Additionalfile2.docx](#)
- [Additionalfile3.tif](#)
- [Additionalfile4.tif](#)
- [Additionalfile5.tif](#)
- [Additionalfile6.xlsx](#)
- [Additionalfile7.pdf](#)
- [Additionalfile8.pdf](#)
- [Additionalfile9.xlsx](#)
- [Additionalfile10.tif](#)
- [Additionalfile11.tif](#)
- [Additionalfile12.tif](#)
- [Additionalfile13.tif](#)